Photon Counting Histogram Analysis as a Tool for Studying the Nature of Intermolecular Interactions

Max Y. Anikovsky and Nils O. Petersen*

National Institute for Nanotechnology, National Research Council and the Department of Chemistry, the University of Alberta, 11421 Saskatchewan Drive, Edmonton, Alberta T6G 2M9, Canada

Received: October 14, 2008; Revised Manuscript Received: January 12, 2009

Photon counting histogram (PCH) analysis is a statistical method that provides independent information about the relative brightness and the number of molecular entities in the system. This suggests that it could be very advantageous in the analysis of intermolecular interactions in multicomponent systems. In this paper we employ PCH to study the interaction of Rhodamine 6G (Rh-6G) with sodium dodecyl sulfate (SDS) micelles and show how the method can unveil the mechanism of quenching of Rh-6G by methyl viologen (MV).

Introduction

Studies of intermolecular interactions followed by photoexcitation have been of enormous interest in the past years. Many reactions occurring in nature are initiated by light and require one or several reactants to be promoted to their excited state. Examining and understanding the mechanisms of these processes are crucial and remain a challenge for scientists. One way to approach this task is through analysis of a fluorescence signal because intermolecular interactions are intrinsically inherent to the process.

Fluorescence intensity depends on two very distinctive parameters: quantum yield and concentration. The photophysical properties of fluorophores determine the quantum yield. Separating the contribution of these two parameters is not always a trivial task. Photon counting histogram (PCH) analysis[1] provides information about the relative brightness and number of fluorescent particles in a volume (concentration), thus effectively determining relative contribution of the photophysical and concentration factors to the overall fluorescent signal. Therefore, PCH may be useful in the analysis of fluorescent quenching which can affect either the quantum yield or the effective concentration.

Mechanisms, by which quenching occurs, span from excited-state reactions to molecular rearrangements.[2] When a decrease in fluorescence intensity is observed due to collisional encounters between a fluorophore in the excited state and a quencher, the process is recognized as *dynamic quenching*. The mechanism suggests that diffusive interaction either opens an additional channel for the excited state to decay, e.g., energy transfer, or accelerates nonradiative paths of energy dissipation, e.g., intersystem crossing. Because all the processes that lead to depopulation of the excited state are competitive, the ensuing outcome is a decrease in the excited-state lifetime of the fluorophore and, consequently, the fluorescence quantum yield.

When the fluorophore and the quencher have high affinity for each other, they can form a stable complex in the ground state. The quencher, when in close proximity, makes the fluorophore virtually nonfluorescent by facilitating nonradiative transitions from the excited state. This mechanism is usually described in terms of the association constant and is known as *static quenching*.

In practical terms, the main difference between dynamic and static quenching is when the interaction between the quencher and the excited state of the fluorophore occurs. In the former case, the fluorophore is initially promoted to its excited state and then interacts with the quencher. In the latter case, the quencher resides in close proximity to the fluorophore prior to excitation.

Both dynamic and static quenching are concentration dependent processes and overall fluorescence intensity decreases with an increase in the quencher concentration. However, the concentration dependence arises from two different effects. In the case of dynamic quenching, higher quencher concentration results in higher probability of collisional interactions with the fluorophore in the excited state and, as a result, lower fluorescence quantum yield of the entire ensemble. In the case of static quenching, the fraction of the population which is completely quenched grows bigger with an increase in the quencher concentration while the remaining, fluorescing ensemble demonstrates no change in the fluorescence quantum yield.

The quenching effect can be conveniently analyzed with Stern−Volmer plots that represent the dependence of fluorescence intensity on the quencher concentration. It has been shown[2] that in the case of both dynamic and static quenching this dependence is linear and, therefore, it is impossible to determine the quenching mechanism based on a single analysis of fluorescence signal intensity at different quencher concentrations. Additional experiments are usually required to determine whether there is a single population of partially quenched molecules (dynamic quenching) or two populations, one fully quenched and one unaffected by quencher (static quenching), or any combination of the above. A frequently encountered approach is the use of lifetime measurements to distinguish between dynamic and static quenching. The observed fluorophore lifetime is affected only when the quenching occurs through dynamic mechanism. In the case of static quenching fluorescence is only observed from unbound emitters and, therefore, their lifetime does not depend on the quencher concentration. Another way to determine the type of quenching mechanism is to carry out fluorescence measurements at different temperatures. Higher temperatures increase collisional rates, making dynamic quenching more efficient. At the same

* Corresponding author. E-mail: Nils.Petersen@nrc-cnrc.gc.ca. Phone: (780) 641 1610. Fax: (780) 641 1601.

10.1021/jp809100a CCC: $40.75
Published on Web 02/25/2009

time the dissociation rates are frequently higher at high temperatures and less static quenching should be observed.[2]

In this paper we show how a single measurement of fluorescence fluctuations over a short period of time can be analyzed by the photon counting histogram (PCH) method to distinguish dynamic and static quenching and determine their relative extent.

We applied the method to a model micellar system. Micelles represent a convenient tool for studying quenching mechanisms at low concentrations. We first examine the complex formation between the fluorescent dye Rhodamine-6G (Rh-6G) and sodium dodecyl sulfate (SDS) micelles. We then determine the type of quenching mechanism arising from interaction of this complex with methyl viologen (MV). The latter is achieved in a single set of PCH experiments.

Experimental Methods

Rh-6G (dye content 99%), SDS (electrophoresis grade, >99% purity), MV dichloride hydrate (98% purity), and methanol (HPLC grade) were purchased from Sigma-Aldrich Canada Ltd. (Oakville, Ontario, Canada) and used without further purification. Aqueous solutions were prepared using deionized water from a Milli-Q water purification system (Millipore, Mississauga, Ontario, Canada).

Raw data for the PCH analysis were collected on an integrated imaging and spectroscopic platform LSM 510 Meta - ConfoCor 2 (Carl Zeiss Canada Ltd., North York, Ontario, Canada). The HeNe laser line (543 nm) was used for Rh-6G excitation. The fluorescence was collected above 605 nm. The data were stored in the Raw Data Format, which gives a true representation of the photon trace and employs a patented data compression technique.[3] Photon counting histograms were retrieved from Raw Data Format files using a constant bin time (10 μs). Each histogram contained 2×10^6 data points. The histograms were later normalized to yield the experimental photon counting probability density plots which in turn were fit to a theoretical PCH model described elsewhere.[4] Calculations were performed using a home developed software operating in MatLab environment (the MathWorks, Inc., ver. R2006a). A function for nonlinear least-squares minimization built as a routine into the MatLab Optimization Toolbox was employed to perform fitting.

For each PCH histogram the procedure yielded three parameters: the number of particles (N), brightness (ε), and correction parameter (F). The parameter F was introduced into the PCH model as a first-order correction for the error arising from collecting photons from non-Gaussian parts of the observation volume profile.[4] Its value should fall into a particular range and can serve as indirect evidence of reliability and reproducibility of the analysis. In the experiments with Rh-6G in methanol, all PCHs were fitted separately. The fitting procedure yielded virtually the same F values with a reasonable magnitude in the expected range.[4] In the case of different dye concentrations and constant laser power, the average value of the correction parameter was 0.5 with the sample variance 2.5×10^{-3}. For PCHs obtained at variable laser powers the average value of F was 0.48 with the sample variance 3×10^{-3}. The sample variance indicates how spread the distribution is and its small values prove that the variability of the correction parameter F is insignificant in both cases, which correlates well with the expectations from the PCH model.

In the PCH analysis of the quenching experiment a global analysis fitting procedure was implemented.[5] Because the correction parameter F did not vary significantly in the analysis of individual histograms, it was used as a single variable in the global analysis fitting. The goodness of the fit was analyzed using reduced χ^2 statistics[2]

$$\chi^2 = \frac{1}{k_{\max} - k_{\min} - n} \sum_{i=k_{\min}}^{k_{\max}} \frac{(P_i - \bar{P}_i)^2}{\sigma_i^2} \qquad (1)$$

where $k_{\max}$ and $k_{\min}$ are maximum and minimum values of the number of photon counts in the histogram, n is the number of fitting parameters (n always equals 3 in our case), P_i is the experimental value in the histogram, $\bar{P}_i$ is the value obtained from the fit, and σ_i^2 is the variance calculated according to a binomial distribution model, $\sigma_i^2 = [P_i(1 - P_i)]/N$, where N is the total number of data points used to build a histogram.

Data for fluorescence correlation spectroscopy (FCS) analysis[6] were collected on the same setup using exactly the same hardware configuration and laser power settings as for the PCH experiments. After the autocorrelation functions were built by the software correlator, they were fit to a theoretical model derived for free three-dimensional diffusion under the assumption that the detection volume is well approximated by a 3D Gaussian function. All the correlation analysis was conducted in the software package provided by Carl−Zeiss with the system. Goodness of the fit was determined by χ_0^2 through the Zeiss software (values of χ_0^2 closest to 0 correspond to the best fit).

The absorption spectra of Rh-6G were recorded on UV−vis spectrophotometer Agilent 8453. The fluorescence spectra of Rh-6G were recorded on Photon Technology International (PTI) MP1 Fluorescence System.

Results

Rh-6G in Micelles. We first describe the behavior of Rh-6G in aqueous solution at a constant dye concentration and different concentrations of SDS. Figure 1 shows the dependence of Rh-6G fluorescence intensity measured at the detector on SDS concentration. The fluorescence increases gradually until the critical micelle concentration (cmc) of 0.008 M is reached.[7] At this concentration the intensity reaches its maximum value and plateaus.

The results of the FCS analysis are presented in Figure 2A. At and slightly above the cmc concentration the Rh-6G diffusion time was measured to be 148 μs, which is approximately 4 times higher than in the absence of SDS (35 μs). The higher value of the diffusion time translates into the diffusion coefficient $D = 0.207 \times 10^{-9}$ m^2 s^{-1}. This agrees well with the value of 0.228×10^{-9} m^2 s^{-1} reported previously for SDS micelles at an SDS concentration of 0.02 M.[8] In both cases, in the absence of SDS and at SDS concentrations higher than the cmc, the autocorrelation function is fit well by one-component model. The one-component model also suffices in the PCH analysis under these experimental conditions. The fitting results are presented in Figure 3 at selected concentrations of SDS. The data suggest that with respect to the fluorescent species the system is homogeneous in the absence of SDS (Figure 3A) and at concentrations where the micelles are formed (Figure 3C,D). We conclude that upon micelle formation, Rh-6G forms a stable complex with SDS micelles. The mean aggregation number measured for SDS micelles just above the cmc varies from 55 to 75 depending on the method.[9] This implies that at the SDS concentration of as low as 0.0084 M (5% above the cmc) the concentration of micelles is expected to be on the order of 6 μM, i.e., several orders of magnitude higher than the concentration of the dye. Statistically we expect that at most one Rh-6G molecule is complexed with any given micelle whereas most micelles do not contain any dye molecules.

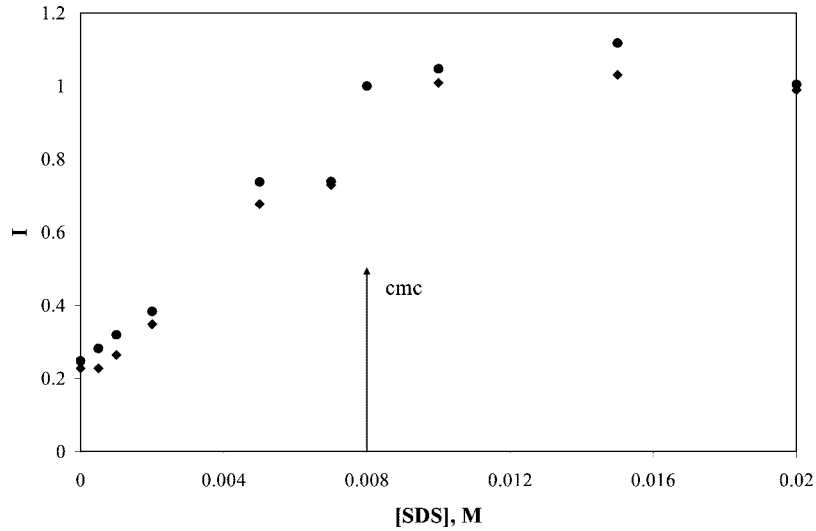

Figure 1. Fluorescence intensity of Rh-6G measured as the detector count rate and normalized at the cmc at different SDS concentrations (diamonds) and fluorescence intensity of Rh-6G calculated by multiplying the molecular brightness on the number of particles, parameters obtained from the PCH fit, and normalized at the cmc (circles). The measurements were conducted at a constant Rh-6G concentration of 3 nM.

The data on the number of particles retrieved by PCH and FCS are presented in Figure 2B. In spite of the fact that the Rh-6G concentration was kept constant in all the experiments, the analyses show that the number of Rh-6G particles in water is half that in micellar solution. To further investigate this observation, we conducted a series of dilution experiments with Rh-6G in water and methanol. In one set of experiments a small volume (1.25% v/v) of a concentrated aqueous stock solution of Rh-6G was added to the equal amounts of methanol and water. Then the number of particles of Rh-6G was measured by FCS. At the second stage of this experiment, the aqueous solution of Rh-6G was removed from the container, pure methanol was added to it, and the FCS measurement was repeated. The analysis revealed presence of the dye in the container in quantities comparable to those in water. See Table 1 for details. This result shows that Rh-6G when dissolved in water gets adsorbed on the walls of the container. When methanol is added, it gets washed off of the walls and transferred into solution.

In a different set of experiments we prepared an aqueous stock solution of Rh-6G and, at the first stage, measured the number of particles in it by FCS. At the second stage we transferred different amounts (% v/v) of Rh-6G from the stock solution into methanol while keeping track of the dilution ratio and then measured the number of particles in the diluted solutions. The main purpose of the experiment was to determine how Rh-6G behavior changes upon transfer from aqueous into alcohol environment. Therefore, volume/volume percentage of water in methanol was kept low to ensure the minimum effect of water on the system. The results presented in Figure 4 show that the number of particles of Rh-6G retrieved by FCS at different dilution factors are higher than expected (dashed line) from the number seen in water. This result is very suggestive that Rh-6G does not exist in purely monomeric form in aqueous solution which contradicts the current views on the aggregation state of Rh-6G in water in the range of nanomolar concentrations.[10] Thus, our data demonstrate that in aqueous solution Rh-6G, in addition to being adsorbed on the walls of a container, is present in suspension in aggregated form.

The PCH brightness analysis is presented in Figure 2C. It shows that, above the cmc, fluorescent species of a constant brightness is observed. This finding supports the notion that the complex in the postmicellar range is formed by monomeric Rh-6G and micelles with the value of Rh-6G brightness twice as big compared to that in water.

One important observation is that the total fluorescence intensity of Rh-6G in SDS micelles measured at the detector is approximately 4 times higher compared to that in water (Figure 1). Interestingly, the number of particles (Figure 2B) and the brightness (Figure 2C) of fluorescent species in the presence of micelles are both twice as big compared to that in water. It appears that the 4-fold increase in intensity arises from twice the number of Rh-6G molecules each with twice the brightness.

The fluorescent spectra of Rh-6G measured in water and SDS above the cmc are presented in Figure 5. The excitation wavelength was 543 nm, and the fluorescence was collected above 605 nm; i.e., the fluorescence excitation and collection conditions were identical to the PCH experiments. The total integrated fluorescence intensity (area under the fluorescence spectrum) was calculated to be twice as high in SDS micelles compared to that in water. For comparison, in the PCH experiments the total fluorescence intensity was 4 times higher in SDS micelles compared to that in water. It is likely that in the range of micromolar concentrations of Rh-6G the surface of a container is saturated with the dye molecules and the overall change in the number of soluble particles due to the dye adsorption on the walls is negligible. As a result, an increase in fluorescence intensity upon transfer of Rh-6G from water into SDS micelles arises mostly from higher brightness of the individual dye molecules. The fluorescence quantum yield of Rh-6G in water was reported to be 0.9.[11] At the same time, the absorption spectra of Rh-6G measured at a constant dye concentration (2×10^{-6} M) in water and SDS above the cmc show that absorbance at the wavelength of excitation (543 nm) is twice as high in SDS compared to that in water (Figure 6). These data suggest that an increase in the fluorescence intensity of Rh-6G and consequently the brightness parameter in the PCH experiment observed upon dye transfer from aqueous into micellar solution occurs as a result of higher extinction at the wavelength of excitation whereas the fluorescence quantum yield remains unaffected as seen from the spectra corrected for absorption (Figure 5, inset).

Rh-6G Interaction with SDS below cmc. Smooth growth of fluorescence intensity observed below the cmc suggests that

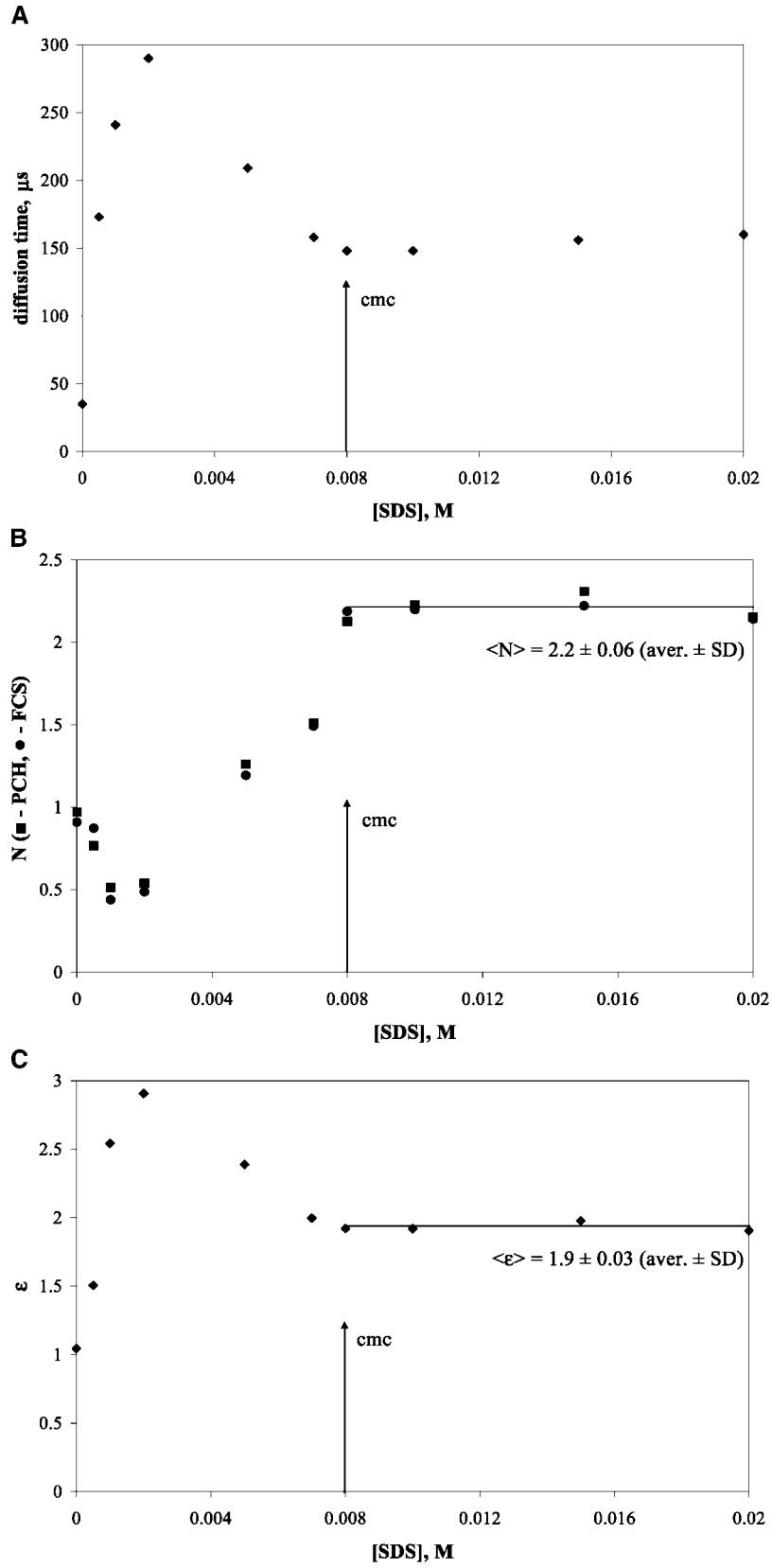

Figure 2. (A) Dependence of Rh-6G diffusion time measured by FCS on SDS concentration. The measurements were conducted at a constant Rh-6G concentration of 3 nM. (B) Results of one-component FCS and PCH analyses for the number of particles of Rh-6G in aqueous solution at different concentrations of SDS. The measurements were conducted at a constant Rh-6G concentration of 3 nM. (C) Results of one-component PCH brightness analysis for Rh-6G in aqueous solution at different concentrations of SDS. The measurements were conducted at a constant Rh-6G concentration of 3 nM.

the surfactant starts interacting with the dye before the micelles are formed. In the range of SDS concentrations below the cmc, the one-component FCS and PCH analyses fail to describe the system with satisfactory preciseness as characterized by the

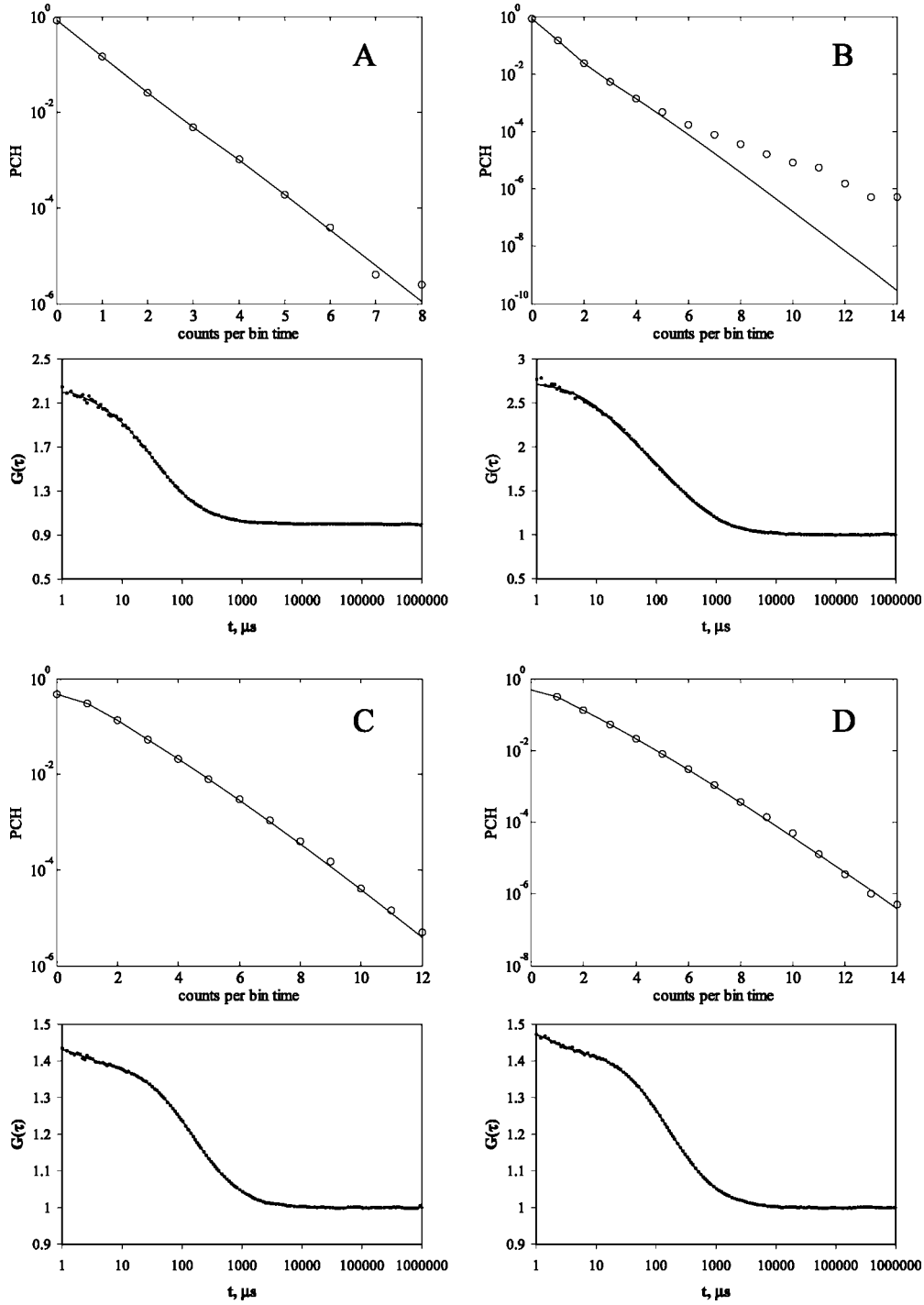

Figure 3. Experimental PCHs and FCS autocorrelation curves with fit at a constant dye concentration and different concentrations of SDS: (A) [SDS] = 0, $\chi^2 = 2.9$ (PCH), $\chi_0^2 = 3.6 \times 10^{-5}$ (FCS); (B) [SDS] = 0.0005, $\chi^2 = 38.9$ (PCH), $\chi_0^2 = 1.3 \times 10^{-4}$ (FCS); (C) [SDS] = 0.008, $\chi^2 = 4.7$ (PCH), $\chi_0^2 = 1.9 \times 10^{-6}$ (FCS); (D) [SDS] = 0.02, $\chi^2 = 2.9$ (PCH), $\chi_0^2 = 1.7 \times 10^{-6}$ (FCS).

values of χ_0^2, χ^2, and F. This is most evident in the PCH curves (Figure 3B). It is interesting, however, that the number of particles retrieved by a one-component PCH model in this range of surfactant concentrations seems to correlate well with the number of particles retrieved by a one-component FCS model (Figure 2B). This, in turn, suggests that in spite of the nonideal fit some useful information may be available in the data. One may note that the diffusion time of Rh-6G below the cmc (Figure 2A) is the mirror reflection of the number of particles retrieved by both FCS and PCH in the same range of surfactant concentrations (Figure 2B). This observation is consistent with

TABLE 1: Number of Rh-6G Particles Measured by FCS in Methanol and Water[a]

N(MeOH) ± SD	N(H_2O) ± SD	N(MeOH after H_2O) ± SD
2.9± 0.02	0.8 ± 0.05	0.75 ±0.05

[a] Number of particles of Rh-6G measured by FCS in methanol (left column) and water (middle column) upon adding equal amounts of the dye from aqueous solution into the solvents. The right column shows the number of particles retrieved by FCS after an aqueous solution of Rh-6G was aspirated and methanol was added to the same container.

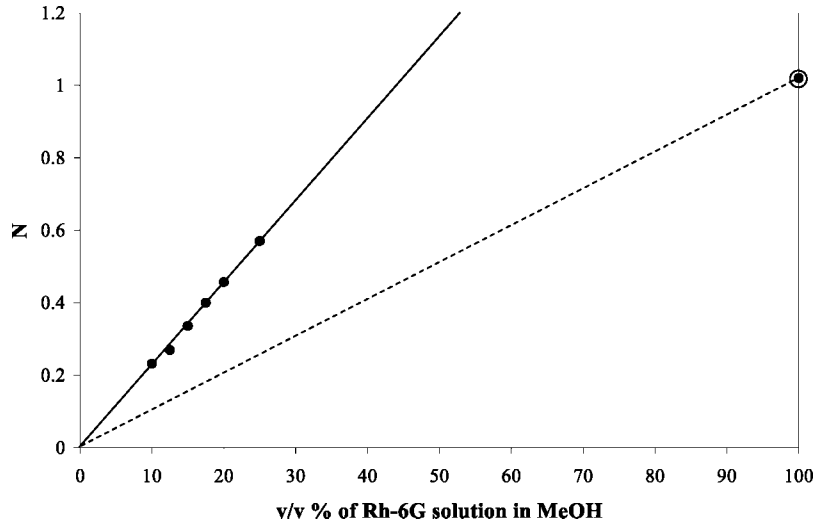

Figure 4. FCS results for the number of particles of Rh-6G in water (the circled dot) and upon dilution of this aqueous stock solution into methanol. The dashed line represents the position where the experimental values of the number of particles were expected to be found on the basis of the dilution factor. The slope of the solid line is more than twice the slope of the dashed line ($k_s = 2.2k_d$).

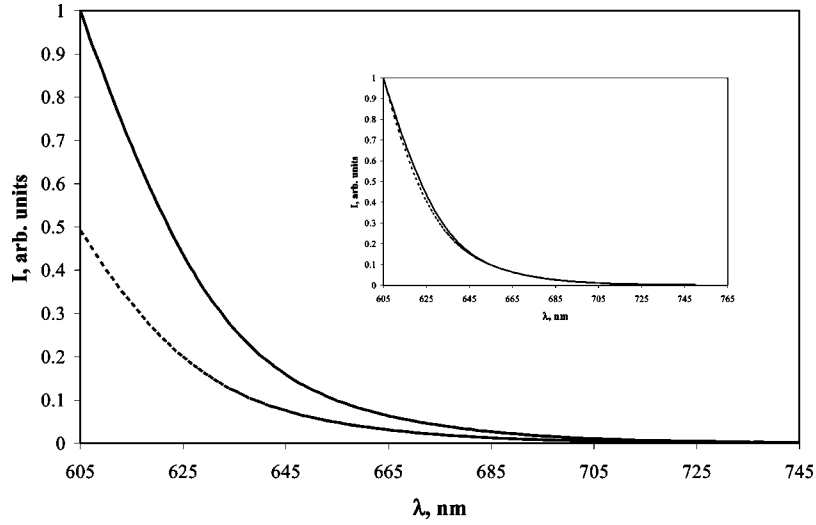

Figure 5. Fluorescence spectra of Rh-6G in water (dotted line) and SDS micelles (solid line) measured at a constant dye concentration (5×10^{-7} M). The wavelength of excitation was 543 nm. The SDS concentration was 2 × cmc (0.016 M). The spectra corrected for absorption are presented in the inset.

the notion that below the cmc SDS and Rh-6G form complexes of variable stoichiometry. These complexes grow in size up to a certain SDS concentration (~0.002 M) as shown by an increase in the diffusion time (Figure 2A) whereas their total number decreases as shown by the values of N (Figure 2B). Past this point, the large complexes start dissociating until the micelles are formed and the system stabilizes. It is very suggestive that the system in the premicellar region is heterogeneous at any given SDS concentration, which is reflected in the nonideality of both FCS and PCH fit below the cmc.

Below the cmc the brightness of fluorescent species increases up to the SDS concentration of 0.002 M and then decreases until the cmc is reached. The result is in accord with the data for the diffusion time and the number of particles. As SDS concentration increases from 0 to 0.002 M, we observe fewer fluorescent species (N decreases, figure 2B) of bigger size (τ_D increases, Figure 2A) comprising more Rh-6G molecules. Consequently, the brightness of these complexes is expected to be increasing as well. Further increase in SDS concentration from 0.002 to the cmc results in the dissociation of the complexes into higher number of smaller aggregates which are becoming less bright due to smaller numbers of Rh-6G molecules comprising them.

Rh-6G Fluorescence Quenched by MV in Micelles. Fluorescence quenching experiments were conducted at constant Rh-6G and SDS concentrations. MV was introduced into the system as a quencher. We expect that in the case of Rh-6G−MV interaction, quenching occurs as a result of electron transfer from the excited fluorophore to MV.[12] The energetics of the process is favorable as seen from the following equation:[13]

$$\Delta G_{el}\,(\text{eV}) = E^0(\text{D}^+/\text{D}) - E^0(\text{A}/\text{A}^-) - \Delta G_{00} = 1.39^{14} - (-0.45^{13}) - 2.27^{14} = -0.4\,\text{eV} \quad (2)$$

Here, ΔG_{el} (eV) is the free energy change for the electron transfer reaction, $E^0(\text{D}^+/\text{D})$ and $E^0(\text{A}/\text{A}^-)$ are oxidation and reduction potentials of the donor and acceptor, respectively, and ΔG_{00} is the free energy corresponding to the equilibrium energy of the excited state relative to the ground state.

Photon counting histograms were obtained for a broad range of the quencher concentrations much larger than the concentra-

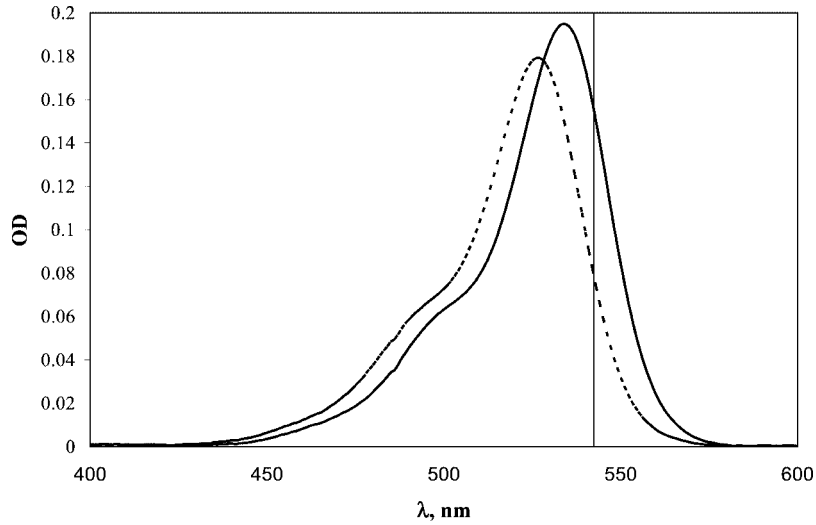

Figure 6. Absorption spectra of Rh-6G measured at a constant dye concentration (2×10^{-6} M) in water (dotted line) and SDS micelles (solid line) at the SDS concentration of 2 × cmc (0.016 M). Vertical line represents the excitation wavelength of 543 nm used in the PCH and FCS experiments.

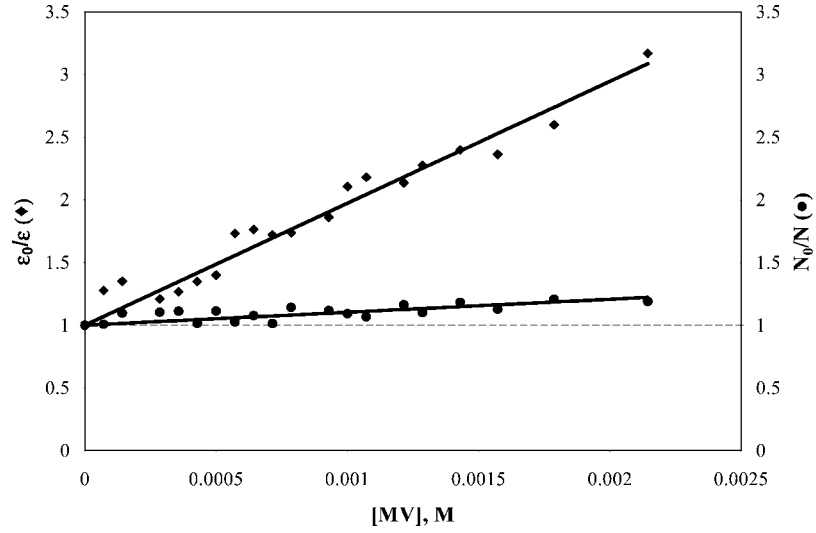

Figure 7. Normalized values of Rh-6G brightness and number of particles at different concentrations of MV. The concentration of Rh-6G was 3 nM and the concentration of SDS was 2 × cmc (0.016 M).

tion of Rh-6G and ranging from about 0.5 to 6.5 MV molecules per micelle. These histograms were then fit using a global analysis procedure to retrieve values of brightness and number of particles for each quencher concentration. The normalized results of the analysis are presented in Figure 7 analogously to the way data are presented in Stern−Volmer plots. It is worth noting that the number of particles retrieved by the PCH analysis correlates well with the number of particles obtained from the FCS analysis (data not shown). By examining the data in Figure 7, one can see that both the brightness parameter and number of particles decrease with an increase in the quencher concentration. The result suggests that quenching occurs by both mechanisms with dynamic quenching responsible for a decrease in the brightness parameter and static quenching responsible for a decrease in the number of particles.

To obtain the dynamic and static quenching constants from the PCH results, we rewrite the dynamic Stern−Volmer equation with values of molecular brightness substituting fluorescence intensities

$$\frac{\varepsilon_0}{\varepsilon} = 1 + k_q\tau_0[Q] = 1 + K_D[Q] \qquad (3)$$

Here ε_0 is the fluorophore brightness in the absence of quencher, k_q is the bimolecular quenching constant, τ_0 is the fluorophore lifetime in the absence of quencher, [Q] is the quencher concentration, and K_D is the dynamic Stern−Volmer constant. Such substitution of fluorescence intensities with the brightness parameters in the Stern−Volmer equation (eq 3) is well justified because fluorescence intensity of a fluorophore is inherent to the brightness parameter by its definition.[1]

Static quenching effectively results in the reduced number of molecules capable of emitting light. In the PCH analysis this is tracked by the number of particles. Substituting the number of particles for the concentrations in the equation for the association constant we obtain

$$\frac{N_0}{N} = 1 + K_S[Q] \qquad (4)$$

Here, N_0 is the number of particles retrieved by the PCH analysis in the absence of quencher and K_S is the association constant for complex formation.

Linear least-squares fitting of eqs 3 and 4 to the experimental data presented in Figure 7 gives the values of dynamic and static quenching constants $K_D = (9.7 \pm 0.5) \times 10^2$ M^{-1} and $K_S = (1.0 \pm 0.2) \times 10^2$ M^{-1}.

Discussion

Rh-6G Interaction with SDS. FCS analysis shows that when SDS reaches the cmc the diffusion coefficient of Rh-6G equals the diffusion coefficient expected to be observed for SDS micelles at this concentration. This change in the diffusion coefficient for Rh-6G compared to that in water indicates that the dye forms a stable complex with the surfactant in a micelle form. One may also note in Figure 2A that a further increase in the surfactant concentration above the cmc increases the diffusion time of the dye slightly. This finding is in good agreement with the fact that, unlike most ionic micelles that have a constant aggregation number, SDS micelles grow in size with an increase in the surfactant concentration.[15] This is consistent with Rh-6G remaining associated with the micelles. Because the micelle concentration is several orders of magnitude higher than the dye concentration, the complex must be uniform and comprise one dye molecule per micelle. The PCH analysis supports this observation.

Applying the one-component model to the experimental PCHs in the postmicellar range is sufficient to obtain fits of high quality as characterized by χ^2 close to 1 and values of the correction parameter F of 0.5. These findings demonstrate that at concentrations above the cmc the system consists of Rh-6G entities with a single brightness, consistent with one monomeric dye molecule in an SDS micelle.

The emission intensity of Rh-6G was found to be higher in the postmicellar region of the surfactant concentrations compared to that in aqueous solutions without SDS, as indicated by the increased value of the detector count rate. Fluorescence enhancement has been observed for many compounds upon their interaction with micelles[16] and has been attributed either to an increased solubilization of dye in micellar solutions[17] or to altered photophysical properties of fluorophores in micelles. The latter is due to changes in the local solvation environment and/or fluorophore shielding in the excited state from quenchers which can be present in the aqueous phase but are insoluble in the micelle.[15]

One of the greatest advantages of the PCH analysis is its ability to determine whether the enhanced fluorescence is caused by higher solubility of the solute, a change in the photophysical properties of the dye, or both. A higher solubility should result in a larger number of particles whereas photophysical properties of the dye should affect the value of the brightness parameter. In this work we find evidence for both higher solubility and altered photophysical properties. The number of particles retrieved by both FCS and PCH methods is twice as high in the postmicellar range as it is in the absence of SDS. This finding suggests that in the absence of the surfactant sparingly soluble Rh-6G molecules adsorb on the walls of the container and/or exist as nonfluorescent nanocrystals in suspension. Our dilution experiments presented in Table 1 and Figure 4 prove that both factors play a role. Indeed, when Rh-6G molecules are transferred from aqueous into alcohol environment, their number did not change proportionally to the dilution factor (Figure 4). On the contrary, for several dilution factors we observe a higher than expected number of molecules in mixtures containing mostly methanol as a solvent compared to aqueous solution. The most reasonable explanation for this effect is that some Rh-6G molecules exist as nonfluorescent entities in water even at nanomolar concentrations. Upon transfer into alcohol environment these aggregates decompose and an increased number of particles is observed. The results of the experiment shown in Table 1 also support this finding. When we add equal amounts of Rh-6G aqueous stock solution to equal volumes of water and methanol, the number of particles measured in methanol is higher compared to that in water. This is very suggestive that not all dye molecules are in the monomeric form in aqueous solution. In addition, Rh-6G molecules are still found in the container after removing the dye aqueous solution from it and adding methanol (Table 1, right column). This experiment proves that Rh-6G indeed adsorbs on the walls of the container which can later be dissolved. SDS micelles have higher solubilization power than water. Therefore, they dissolve the aggregated structures present in water and incorporate monomeric dye molecules which results in higher number of molecules measured by PCH and FCS in micelles compared to that in water.

At the same time the molecular brightness of Rh-6G was found to be 2 fold higher above the cmc compared to that in aqueous solutions without SDS. This would not be observed if dye molecules are simply desorbed from the walls and/or suspension. Thus, interaction of Rh-6G with micelles formed by SDS, in addition to higher solubilization, results in an enhanced emission caused by higher extinction of the dye at the excitation wavelength.

The behavior of Rh-6G at SDS concentrations below the cmc is more complex. One-component FCS analysis detects up to a 7-fold increase in the diffusion time of the dye. We believe that this effect is due to an association between the dye and SDS molecules. Such aggregation in the premicellar solutions has been observed previously for other dyes. For instance, it has been shown that both cationic and anionic cyanine dyes form mixed dye−SDS aggregates below the cmc.[18,19] It should be noted that these aggregates are heterogeneous and contain different numbers of dye and SDS molecules at any given SDS concentrations. This conclusion arises from the FCS and PCH analyses of these solutions. In both cases one-component analysis fails to describe the data with satisfactory preciseness, suggesting that aggregates of different order are present in each solution. Micelle formation stabilizes the system and causes the aggregates to form micelles some of which contain a single Rh-6G molecules. The poor fits for PCH and FCS in the premicellar region make it difficult to rely on the values for D, N, and ε (Figure 3). Nevertheless, it is interesting to observe that the fluorescence intensity calculated as the molecular brightness multiplied by the number of particles follows the same trend as the fluorescence intensity measured at the detector (Figure 1), indicating that the parameters retrieved from PCH are meaningful in spite of the poor fits. Moreover, the changes in D, N, and ε in the premicellar region are consistent with a formation of a smaller number (N) of large (D) and bright (ε) structures up to the surfactant concentration of ~ 0.002 M SDS or one-fourth the cmc and further dissociation of these structures into higher number (N) of smaller (D) and less bright (ε) entities until the system stabilizes at the cmc. It is important that the minimum number of particles (N_{min}) occurs at the same concentration where the largest (D_{max}) and brightest (ε_{max}) particles are observed.

MV Interaction with Rh-6G in SDS Micelles. In our PCH experiment we observe a decrease in both the brightness and the number of particles (Figure 7). This result implies that both dynamic and static mechanisms are engaged in the quenching process. The dynamic quenching constant was found to be an order of magnitude higher than its static counterpart showing that the dynamic quenching is dominant over the static one. Frequently, the efficiency of the dynamic quenching or the accessibility of the fluorophore to the quencher is evaluated by the value of the bimolecular quenching constant:

$$k_q = \frac{K_D}{\tau_0} \quad (5)$$

where τ_0 is the lifetime of the fluorophore in the absence of quencher. For Rh-6G in SDS micelles τ_0 is 4.6 ns[20] and, consequently, the bimolecular quenching constant was evaluated to be $k_q = 2.2 \times 10^7\ M^{-1}\ s^{-1}$.

It is often useful to compare the bimolecular quenching constant to the diffusion controlled bimolecular rate constant, which can be calculated using the Smoluchowski equation. The diffusion controlled bimolecular rate constant may be viewed as the largest possible rate at which quenching can occur in solution. Its value is usually near $1 \times 10^{10}\ M^{-1}\ s^{-1}$. However, when the diffusion of the fluorophore or quencher is slowed, smaller values of the diffusion controlled bimolecular rate constant are expected. In our experiment due to complex formation between Rh-6G and SDS the fluorophore diffuses with the diffusion rate of the micelles. This, in turn, results in a reduced value of the diffusion controlled bimolecular rate constant for the system which we estimated to be $6 \times 10^9\ M^{-1}\ s^{-1}$. This value is more than 2 orders of magnitude higher than the bimolecular quenching constant measured in the experiment. Lower values of the bimolecular quenching constant compared to the diffusion controlled bimolecular rate constant is usually a result of ineffective quenching; i.e., not every collision of the quencher with the fluorophore in the excited state results in quenching, or high degree of steric shielding of the fluorophore. It is possible that such shielding occurs as a result of different binding nature of the fluorophore and quencher with the micelles.

Conclusions

PCH proved to be a powerful tool for studying molecular dynamics. Its ability to separate the molecular brightness and number of particles allowed us to show that upon interaction of Rh-6G with SDS micelles an increase in the fluorescence intensity is observed not only due to changes in molecular microenvironment but also because of an increased solubility of the dye in the micellar solution. The method proved to be extremely useful when studying fluorescence quenching. It allows determination of the quenching mechanism and relative contribution of the dynamic and static components if both are present in the system through a single measurement.

Acknowledgment. The work was supported by CIPI and NSERC. We thank Dr. Xuejun Sun and Ms. Gerry Barron at Cell Imaging Facility, Department of Oncology, the University of Alberta, and Cross Cancer Institute for technical assistance.

References and Notes

(1) Chen, Y.; Muller, J. D.; So, P.; Gratton, E. *Biophys. J.* **1999**, *77*, 553–567.
(2) Lakowicz J. *Principles of fluorescence spectroscopy*; Springer: New York, Berlin, 2006.
(3) Weisshart, K.; Jüngel, V.; Briddon, S. J. *Curr. Pharm. Biotech.* **2004**, *5*, 135–154.
(4) Huang, B.; Perroud, T. D.; Zare, R. N. *Phys. Chem. Chem. Phys.* **2004**, *5*, 1523–1531.
(5) Beechem J. M.; Gratton E.; Ameloot M.; Knutson J. R.; Brand L. The global analysis of fluorescence intensity and anisotropy decay data: second generation theory and programs. In *Topics in Fluorescence Spectroscopy: Principles*; Plenum Press: New York, 1991; Vol. 241, p 306.
(6) Elson, E. L.; Magde, D. *Biopolymers* **1974**, *13*, 1–27.
(7) Bales, B. L.; Messina, L.; Vidal, A.; Peric, M. *J. Phys. Chem. B* **1998**, *102*, 10347–10358.
(8) Ribeiro, A. C. F.; Lobo, V. M. M.; Azevedo, E. F. G.; da G. Miguel, M.; Burrows, H. D. *J. Mol. Liq.* **2003**, *102*, 285–292.
(9) Yoshii, N.; Iwahashi, K.; Okazakia, S. *J. Chem. Phys.* **2006**, *124*, 184901.
(10) (a) Toptygin, D.; Packard, B. Z.; Brand, L *Chem. Phys. Lett.* **1997**, *277*, 430–435. (b) Jahanbakhsh Ghasemi, J.; Niazi, A.; Kubista, M. *Spectrochim. Acta Part A* **2005**, *62*, 649–656.
(11) Magde, D.; Wong, R.; Seybold, P. G. *Photochem. Photobiol.* **2002**, *75*, 327–334.
(12) Qu, P.; Zhao, J.; Shen, T.; Hidaka, H. *J. Mol. Catal. A: Chem.* **1998**, *129*, 257–268.
(13) Kavarnos G. J. *Fundamentals of Photoinduced Electron Transfer*; VCH Publishers, Inc.: New York, 1993.
(14) Heinlein, T.; Knemeyer, J.-P.; Piestert, O.; Sauer, M. *J. Phys. Chem. B* **2003**, *107*, 7957–7964.
(15) Bales, B. L.; Almgred, M. *J. Phys. Chem.* **1995**, *99*, 15153–15162.
(16) Georges, J. *Spectrochim. Acta Rev.* **1990**, *13*, 27–45.
(17) Minch, M. J.; Shah, S. S. *J. Org. Chem.* **1979**, *44*, 3252–3255.
(18) Tatikolov, A. S.; Costa, S. M. B. *Chem. Phys. Lett.* **2001**, *346*, 233–240.
(19) Vinogradov, A. M.; Tatikolov, A. S.; Costa, S. M. B. *Phys. Chem. Chem. Phys.* **2001**, *3*, 4325–4332.
(20) Klein, U. K. A.; Haar, H. P. *Chem. Phys. Lett.* **1978**, *58*, 531–536.

JP809100A